JOURNAL OF SCIENCE
SAKARYA UNIVERSITY

Sakarya University Journal of Science

ISSN 1301-4048 | e-ISSN 2147-835X | Period Bimonthly | Founded: 1997 | Publisher Sakarya University | http://www.saujs.sakarya.edu.tr/

Title: Comparison Of Reversible Image Watermarking Methods Based On Prediction-Errors

Authors: Emre Altınkaya, Burhan Baraklı
Recieved: 2018-10-02 00:00:00

Accepted: 2018-10-02 00:00:00

Article Type: Research Article
Volume: 23
Issue: 4
Month: August
Year: 2019
Pages: 493-500

How to cite
Emre Altınkaya, Burhan Baraklı; (2019), Comparison Of Reversible Image Watermarking Methods Based On Prediction-Errors. Sakarya University Journal of Science, 23(4), 493-500, DOI: 10.16984/saufenbilder.466656
Access link
http://www.saujs.sakarya.edu.tr/issue/43328/466656

Sakarya University Journal of Science 23(4), 493-500, 2019

Comparison Of Reversible Image Watermarking Methods Based On Prediction-Errors

Emre ALTINKAYA*[1], Burhan BARAKLI[2]

Abstract

This study compares two reversible image watermarking algorithms applied to a digital image. The first algorithm is a method based on adaptive watermarking of prediction-errors. With this method, as in the existing reversible image watermarking methods, pixels are embedded in two different ways according to the values of prediction-errors instead of applying the same watermarking algorithm to all pixels in the imageAccordingly, the image pixels are divided into two blocks as uniform and non-uniform. The watermarking capacity has been increased by embedding 2-bit to specific pixels of uniform blocks and 1-bit to specific pixels of non-uniform blocks. The second algorithm is a method based on interpolation errors. In this method, interpolation error is utilized. The two methods compared with each other were compared with the existing methods in the literature by using computer simulations, and superior and weak aspects of the methods were determined.

Keywords: reversible watermarking, adaptive reversible image watermarking, pixel selection, prediction-error expansion, interpolation error expansion

1. INTRODUCTION

Various coding techniques are used for the reliability of the data in digital media. However, cryptography is not solely adequate to protect the data. In this context, digital watermarking is a complementary method for cryptography by eliminating the lack of cryptography for the reliability of data. Digital watermarking is frequently used in applications such as data control, secure data transfer and data hiding. Digital watermarking has an undesirable side effect along with its benefits. This side effect is the damage of watermark to the original data that it has been embedded to. The method used in the situations, where data corruption is not desired and the original watermark is desired to be recovered from the watermarked correctly, is called reversible watermarking (RW). Reversible watermarking is a special method of hiding data. The original data can be obtained after extracting the embedding with the recycling feature. RW can be performed for many digital signals; however, it is mostly used in digital image applications. By using the RW method, the watermark is removed from an image that is desired to be watermarked and also the original image is recovered with intrinsic accuracy.

* Corresponding Author: mr.altinkaya@gmail.com
[1] Sakarya University, Electrical and Electronics Engineering, Sakarya, TURKEY. ORCID: 0000-0003-3172-1591
[2] Sakarya University, Electrical and Electronics Engineering, Sakarya, TURKEY. ORCID: 0000-0002-7947-2312

Thanks to this advantage, RW has an important place in image watermarking applications. For example, it is considerably beneficial in military, medical and remote sensing applications.

The success of RW is determined by examining three important conditions in watermarking: similarity, capacity and robustness. Similarity can be defined as perceptual similarity between the original and watermarked data. Capacity is the maximum amount of information that can be stored in the original data. Robustness is the ability to obtain watermark from the watermarked data in bad intention or in other cases. In the applications, the parameters are determined according to the situation with higher priority and the algorithm is developed accordingly.

When examining the existing RW algorithms found in the literature review, the old methods are based on lossless compression. These methods generally have low capacity and cause severe degradation in the image quality. Considering these problems, more efficient algorithms have been developed to increase the capacity and minimize the degradation in further studies. In this context, three basic methods stand out: prediction-error expansion (PEE) by Thodi et al. [4, 5], histogram shifting (HS) by Ni et al. [6, 7], and difference expansion (DE) by Tian et al. [8]. Among these methods, the PEE technique attracts more attention because it can create better spaces in the image compared to others. In our literature research, in addition to the methods mentioned above, the following topics which are popular in recent years are examined. This topics: wavelet-based image watermarking technique by Khelifi et al. [9], A new 4-D chaotic hyperjerk system, its synchronization, circuit design and applications in RNG, image encryption and chaos-based steganography by Vaidyanathan et al. [10], A low complexity video watermarking in H. 264 compressed domain by Mansouri et al. [11], and A new two-level data hiding algorithm for high security based on a nonlinear system by Akgul et al. [12].

In the first method proposed by Thodi and Rodriguez, prediction error is used instead of difference value for the expansion embedding [4]. In the image watermarking method using the PEE technique, two different methods stand out when obtaining the prediction image and adding the embedding. They are based on interpolation and adaptive watermarking. In these methods, more

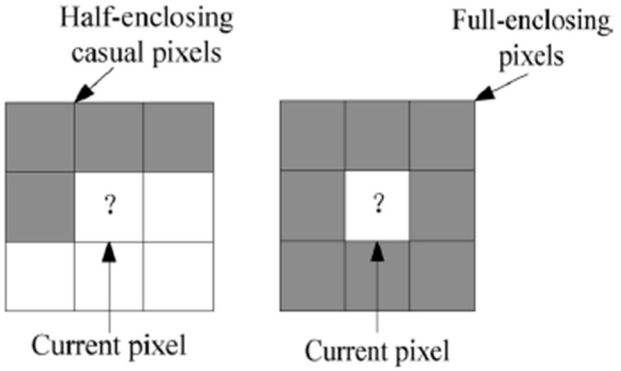

Fiure 1. Half-enclosing and full-enclosing casual pixels [14]

neighborhood relations are used instead of two adjacent pixels. In addition, Thodi and Rodriguez suggest combining histogram shifting and expansion embedding in RW. Many other methods based on PEE have been proposed [13, 14]. There are differences in the prediction algorithms used in these methods.

This article compares the interpolation and adaptive watermarking based methods. The comparison is made for various numbers of embeddings and different images. In order to compare the performance of the methods, the number of bits per pixel (BPP) and the peak signal-to-noise ratio (PSNR) have been used. The rest of the article is organized as follows:

2. INFRASTRUCTURE

The method based on the interpolation error and the method based on the adaptive expansion of the prediction error have an important place in RW and they are used effectively. In this section, two methods to be compared in this article will be examined.

2.1. RW based on Interpolation Error

Interpolation is to approximately obtain the unknown intermediate values using the sample data obtained. In the method to be discussed in this section, the prediction image used in the watermarking is obtained by the interpolation technique.

This technique utilizes the correlation between image pixels more effectively. The interaction between pixels is seen in Figure 1. Thanks to the correlation between pixels, this method outperforms some existing methods.

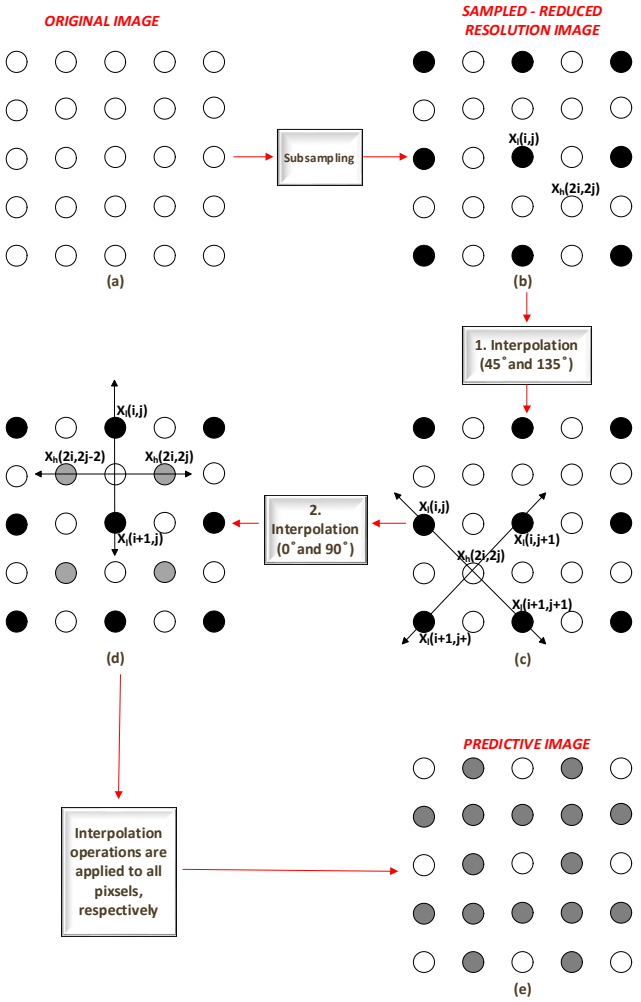

Figure 2. (a) Original image, (b-c) The formation of low-resolution image x_1 from high-resolution image x_h, (d) Interpolation of residual samples of high-resolution, (e) The interpolation of the sample pixels

When some existing methods use half-enclosing pixels as in Figure 1, full-enclosing pixels are used in interpolation method. Thus, more accurate values are obtained by increasing the correlation between pixels.

An appropriate image interpolation algorithm is described below to obtain the interpolation values and errors. Image interpolation is the process of producing a high-resolution image from its low-resolution image equivalent. When the method is examined, the interpolation algorithm of Zhang et al. [15] is utilized. In Figure 2, x_l is a low-resolution image while x_h is a high-resolution image. The equation $x_l(i,j) = x_h(2i-1,2j-1)$ is sampled with $1 \le i \le N$ and $1 \le j \le M$. In Figure 2(b), the black points indicate the pixels of x_l while the white points indicate the missing pixels of x_h. To predict x_h, the value with two interpolations is combined with the most appropriate weight pair. The high-resolution x_h is regenerated at two steps. First, the missing pixels of $x_h(2i,2j)$, which is located at central points

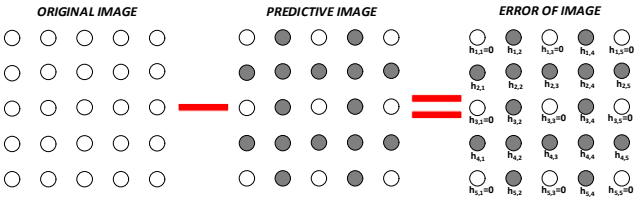

Figure 3. Determination of interpolation error

surrounded by low-resolution pixel, are subject to interpolation. Secondly, other missing pixels, $x_h(2i-1,2j)$ and $x_h(2i,2j-1)$, are subject to interpolation with the help of previously recovered pixel $x_h(2i,2j)$.

Considering Figure 2(c), interpolation is made for $x_h(2i, 2j)$ according to 45^0 diagonal and 135^0 diagonal pixel values.

Interpolation values in both directions indicated as $\bar{x}_{45}(2i,2j)$ and $\bar{x}_{135}(2i,2j)$ are as shown below:

$$\begin{cases} \bar{x}_{45} = (x_l(i,j+1) + x_l(i+1,j))/2 \\ \bar{x}_{135} = (x_l(i,j) + x_l(i+1,j+1))/2 \end{cases} \quad (1)$$

Interpolation errors, h_{45} and h_{135} values, are calculated as follows:

$$\begin{cases} h_{45}(2i,2j) = \bar{x}_{45}(2i,2j) - x_h(2i,2j) \\ h_{135}(2i,2j) = \bar{x}_{135}(2i,2j) - x_h(2i,2j) \end{cases} \quad (2)$$

Instead of calculating the linear minimum mean square error prediction of x_h, optimum weight pair is selected to predict $\bar{x}_h$ from x_h.

$$\begin{cases} \bar{x}_h = w_{45} \bullet \bar{x}_{45} + w_{135} \bullet \bar{x}_{135} \\ w_{45} + w_{135} = 1 \end{cases} \quad (3)$$

w_{45} and w_{135} weight values minimize the mean square error of x_h.

$$\{w_{45}, w_{135}\} = arg_{w_{45}+w_{135}=1} \min E[(\bar{x}_h - x_h)^2] \quad (4)$$

$$w_{45} = \frac{\sigma(h_{135})}{\sigma(h_{45})+\sigma(h_{135})}, \quad w_{135} = 1 - w_{45} \quad (5)$$

where $\sigma(h_{45})$ and $\sigma(h_{135})$ values are variance predictions of h_{45} and h_{135} values, respectively. Equation (5) explains the working mechanism of weighting calculations. For example, for an edge in the direction or near 45^0 diagonal, $\sigma(h_{135})$ is higher than $\sigma(h_{45})$, thus w_{135} becomes smaller than w_{45}. As a result, $\bar{x}_{135}$ has less effect on $\bar{x}_h$ rather than $\bar{x}_{45}$. Similarly, the opposite is also valid.

Considering Figure 2(c), the mean value of $x_h(2i, 2j)$ is indicated as u and predicted using low-resolution pixels around $x_h(2i, 2j)$.

$$u = \frac{(x_l(i,j+1)+x_l(i+1,j))}{4} + \frac{(x_l(i,j)+x_l(i+1,j+1))}{4} \quad (6)$$

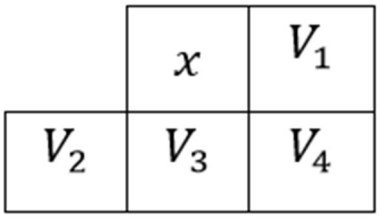

Figure 4. The pixels used for prediction calculation of a pixel

The variance predictions of interpolation errors are calculated as follows:

$$\begin{cases} \sigma(h_{45}) = \frac{1}{3}\sum_{k=1}^{3}(S_{45}(k) - u)^2 \\ \sigma(h_{135}) = \frac{1}{3}\sum_{k=1}^{3}(S_{135}(k) - u)^2 \end{cases} \quad (7)$$

$$\begin{cases} S_{45} = \{x_l(i, j+1),\ \bar{x}_{45},\ x_l(i+1, j)\} \\ S_{135} = \{x_l(i, j),\ \bar{x}_{135},\ x_l(i+1, j+1)\} \end{cases} \quad (8)$$

To obtain the predictions of the unknown high-resolution pixel $x_h(2i, 2j)$, first Equations (1) - (8) are used. The pixel values $x_h(2i-1, 2j)$ and $x_h(2i, 2j-1)$ left after the prediction of $x_h(2i, 2j)$ are similarly predicted.

Considering Figure 2(d), the black dots indicate low-resolution pixels, gray dots indicate the predictive pixels at the first step and white dots indicate the pixels to be interpolated. These operations are the same as those in the first step but the directions are 0^0 and 90^0. These operations are applied to all pixels, respectively.

Figure 3 shows how the image error is obtained. The error of the pixels used in the operations was obtained by removing the predictive image obtained with the operations in Figure 2 from the original image. All errors are seen as the image errors.

2.2. Adaptive Watermarking based RW

To apply the examined technique (adaptive watermarking) to the image, first the prediction of the image is created using an appropriate prediction method. The median edge detector (MED) method used by Thodi and Rodriguez in the literature is used to create the prediction [16]. The pixels used in the calculations in this method are shown in Figure 4.

The prediction of x pixel indicated as $\bar{x}$ is calculated using the below equation:

$$\bar{x} = \begin{cases} \min(V_1, V_3), & V_4 \geq \max(V_1, V_3) \\ \max(V_1, V_3), & V_4 \leq \min(V_1, V_3) \\ V_1 + V_3 - V_2, & other\ cases \end{cases}$$

In the technique discussed above, the prediction method used in the present study is seen. After obtaining the prediction of the image, the prediction error is obtained using the equation $h = x - \bar{x}$. When these operations are applied for all pixels, the prediction error of the image is determined. After finding the prediction error, adaptive watermarking steps can be applied.

In adaptive watermarking, the image is divided into two parts as uniform and non-uniform regions, unlike existing classical methods that embed the data in an equal and uniform way. 2 bits is embedded to each expandable pixel in the uniform region while 1 bit is embedded to those in the non-uniform region. This prevents the pixels from expanding with high prediction errors when the capacity is high and also decreases the embedding effect by reducing the maximum change to the pixel values.

When a pixel is embedded with 1 bit, the mean distortion occurred in pixels can be calculated with the below equation:

$$B_1(h) = E[(I^d(i,j) - I(i,j))^2] \quad (9)$$

where,

$I^d = \bar{I} + h^d$,

$I^d = (I - h) + (2h + b)$,

$I^d = I + h + b$,

Putting above equation into Equation (9), the following equation is obtained.

$$E\left[\left(I^d(i,j)-I(i,j)\right)^2\right]=E[(I+h+b-I)^2],$$
$$=E[(h+b)^2] \quad (10)$$

When calculating this equation, the mean distortion is obtained as follows:

$$B_1(h)=E[(h+b)^2]=\frac{1}{2}\sum_{b\mathcal{E}\{0,1\}}(h+b)^2$$
$$=h^2+h+0{,}5 \quad (11)$$

When the prediction error is embedded with 2 bit, the calculation of the mean distortion in pixels is as follows (in 2 bit embedding, $b_1, b_2 \mathcal{E}\{0,1\}$):

Watermarked pixel value is calculated using the below equation:

$$I^d=\bar{I}+2(2h+b_1)+b_2=\bar{I}+4h+2b_1+b_2$$
$$=I+3h+2b_1+b_2$$

The mean distortion is obtained as follows:

$$\left[\left(I^d(i,j)-I(i,j)\right)^2\right]$$
$$=E[(I+3h+2b_1+b_2-I)^2]$$
$$=E[(3h+2b_1+b_2)^2],$$
$$B_2(h)=E[(3h+2b_1+b_2)^2]$$
$$=\frac{1}{4}\sum_{b_1,b_2\mathcal{E}\{0,1\}}(3h+2b_1+b_2)^2$$
$$=9h^2+9h+3{,}5 \quad (12)$$

Examining Equations (11) and (12), when the prediction errors are the same, embedding a pixel with 2 bit causes more distortion than that with 1 bit ($B_2(h)\geq B_1(h)$). However, if prediction errors are different and $|h_1|$ is sufficiently larger than $|h_2|$, then $B_1(h_1)>B_2(h_2)$. Therefore, h_1 with its sufficient magnitude can cause more distortion in 1 bit embedding. When these cases are considered, embedding a pixel having less prediction error with 2 bit causes less distortion compared to embedding a pixel having sufficiently high prediction error with 1 bit.

To classify which pixels are in the uniform region and those are in the non-uniform region in adaptive watermarking, standard deviation forward variance (FV) calculated utilizing the neighbourhood relations of image pixels [17]. FV calculation is shown in Equation (13).

$$FV=\sqrt{\frac{1}{4}\sum_{k=1}^{4}(V_k-\bar{V})^2} \quad (13)$$

$$V_k=\{V_1,\dots,V_4\}, \qquad \bar{V}=\frac{1}{4}\sum_{k=1}^{4}V_k$$

The positions of pixel values used for the FV calculation in Equation (13) are shown in Figure4.

The pixels having less FV than adaptive watermarking threshold value ($\triangle_{tae}$) are called uniform while those having a FV higher than $\triangle_{tae}$ are called non-uniform [17]. The pixels with low prediction error in the uniform region can be embedded with 2 bit while those with high prediction error in the non-uniform region can be embedded with 1 bit.

3. RESULTS

In this article, RW methods based on the interpolation and the adaptive watermarking of the prediction error have been compared. In addition to the results of these two methods discussed in the article, the data of some methods examined in the literature studies have been also added and compared.

Figure 5. Lena and Sailboat images

In the methods studied in the literature studies, the method by Lin et al. was about lossless data hiding based on DE without location map. Tsai et al. carried out a study on the reversible image hiding scheme with the predictive coding and histogram shifting characteristic. H.-J Kim et al. developed and implemented a new DE transformation method for reversible data embedding. K.-S. Kim et al. developed a reversible data hiding method that can be

exploited from the spatial correlation between subsample images.

Software for empirical studies of the methods compared in this article was performed on MATLAB. The watermarks to be added come from random arrays created by the software. The methods examined in the article were applied to 512x512 Lena and Sailboat images as shown in Figure 5.

Bit per pixel (BPP) and peak-to-signal noise ratio (PSNR) were used to compare the performance of methods.

N_g is the number of bit added to the image while M and N values are width and length of the image in terms of pixels, respectively. BPP can be calculated as follows:

$$BPP = \frac{N_g}{M\ x\ N} \tag{14}$$

PSNR values indicating the image quality are calculated as desibel using the below equation:

$$PSNR = 10log\left(\frac{255\ x\ 255}{\sum_{i=1}^{M}\sum_{j=1}^{N}\left(I(i,j)-I^{d}(i,j)\right)^{2}}\right) \tag{15}$$

Capacity (BPP) – PSNR (dB) performance graphs obtained for both images are shown in Figures 6 and 7.

The following results can be deduced from the graphical curves of Figures 6 and 7 obtained as the experimental data. First, as the amount of added watermark (bit) increases, the image quality of the methods decreases. In addition, in some methods this decline has been sudden and

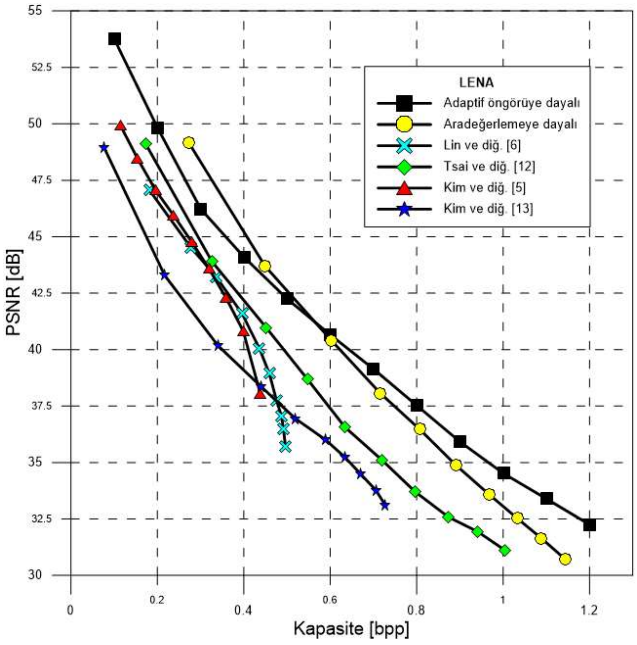

Figure 6. The performance of the existing and suggested methods for the Lena image

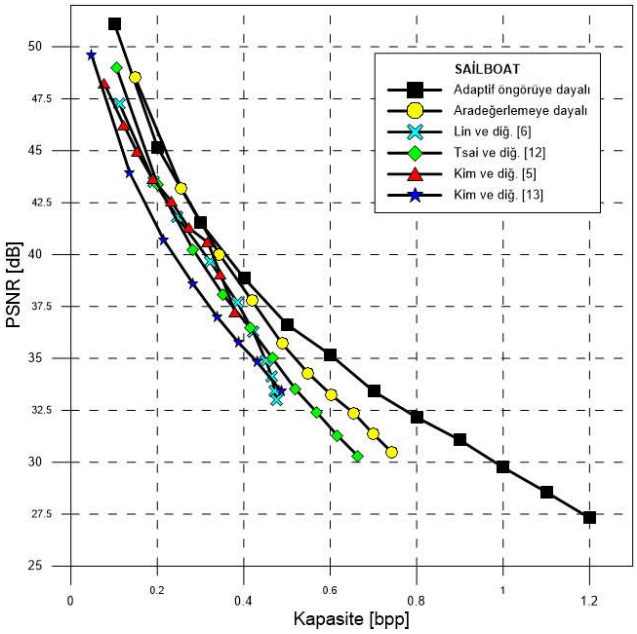

Figure 7. The performance of existing and suggested methods for the Sailboat image

severe. The reason for this is that the capacity parameter determined to provide the capacity could not satisfy the amount of watermark.

Secondly, the methods used for comparison are not adaptive. When comparing the data obtained using the adaptive method with those obtained using non-adaptive methods discussed in Section 2.2, adaptive watermarking gives higher capacity and better image quality. For example, the proposed method achieved a visual quality gain of

3 dB and 3.5 dB for Lena and Sailboat images, respectively, at a level of 0.6 bpp when compared to the method by Tsai et al.

Figure 8. Watermarked images

It is also possible to watermark at very high bpp levels with the adaptive method. As can be seen from the graphs, it is possible to watermark at values higher than 1 bpp by the proposed method while it is possible to watermark at lower bpp values by the comparative methods. Third, the performance of the methods is affected by the shape of the histograms of images. The methods produce similar results in the image with uniformly distributed histogram. This is exemplified by the performances up to 0.4 bpp in the Lena image and up to 0.3 bpp in the Sailboat image.

Lastly, we find out that interpolation-based method provides better visual quality at low capacity levels when comparing the interpolation-based method discussed in Section 2.1 and the adaptive watermarking based method. However, as the amount of watermark increases, the effect of adaptive watermarking on the watermarking is better than other methods. Thus, both high capacity and better visual quality values can be achieved with adaptive watermarking method. For example, if the graph obtained for the sailboat image is examined, the data obtained by the adaptive watermarking method can reach 1.2 bpp, while the data obtained with the interpolation method remains at 0.7 bpp. Examining the image quality of 0.6 bpp for the same image, the proposed adaptive method provides about 2.5 dB better visual quality than the interpolation method.

Figure 8 shows the watermarked images of Lena and Sailboat images at 0.1 and 1.2 bpp levels obtained using the examined adaptive watermarking method.

REFERENCES

[1] J. M. Barton, “Method and Apparatus for Embedding Authentication Information Within Digital Data,” U.S. Patent 5 646 997, 1997.

[2] C. I. Podilchuk, E. J. Delp, “Digital Watermarking: Algorithms and Applications,” July, pp. 33–46, 2001.

[3] B. Furht, E. Muharemagic, D. Socek, “Multimedia Encryption and Watermarking. Springer. ”

[4] D. M. Thodi and J. J. Rodriguez, “Expansion embedding techniques for reversible watermarking,” IEEE Trans. Image Process., vol. 16, no. 3, pp. 721–730, Mar. 2007.

[5] W. Hong, T. S. Chen, and C. W. Shiu, “Reversible data hiding for high quality images using modification of prediction errors,” J. Syst. Softw., vol. 82, no. 11, pp. 1833–1842, Nov. 2009.

[6] Z. Ni, Y. Q. Shi, N. Ansari, and W. Su, “Reversible data hiding,” IEEE Trans. Circuits Syst. Video Technol., vol. 16, no. 3, pp. 354–362, Mar. 2006.

[7] S. K. Lee, Y. H. Suh, and Y. S. Ho, “Reversible image authentication based on watermarking,” in Proc. IEEE ICME, 2006, pp. 1321–1324.

[8] J. Tian, “Reversible data embedding using a difference expansion,” IEEE Trans. Circuits Syst. Video Technol., vol. 13, no. 8, pp. 890–896, Aug. 2003.

[9] F. Khelifi, A. Bouridane, F. Kurugollu and A. I. Thompson, “An improved wavelet-based image watermarking technique,” IEEE Conference on Advanced Video and

Signal Based Surveillance, 2005., Como, 2005, pp. 588-592.

[10] S. Vaidyanathan, A. Akgul, S. Kaçar and U. Çavuşoğlu "A new 4-D chaotic hyperjerk system, its synchronization, circuit design and applications in RNG, image encryption and chaos-based steganography," Eur. Phys. J. Plus 133: 46 (2018).

[11] A. Mansouri, A. M. Aznaveh, F. Torkamani-Azar and F. Kurugollu, "A Low Complexity Video Watermarking in H.264 Compressed Domain," in IEEE Transactions on Information Forensics and Security, vol. 5, no. 4, pp. 649-657, Dec. 2010.

[12] A. Akgul, S. Kacar, and B. Aricioglu, "A new two-level data hiding algorithm for high security based on a nonlinear system," Nonlinear Dyn 90: 1123 (2017).

[13] M. Fallahpour, "Reversible image data hiding based on gradient adjusted prediction," IEICE Electron. Express, vol. 5, no. 20, pp. 870–876, Oct. 2008.

[14] L. Luo, Z. Chen, M. Chen, X. Zeng, and Z. Xiong, "Reversible image watermarking using interpolation technique," IEEE Trans. Inf. Forensics Security, vol. 5, no. 1, pp. 187–193, Mar. 2010.

[15] L. Zhang and X. Wu, "An edge-guided image interpolation algorithm via directional filtering and data fusion," IEEE Trans. Image Process., vol. 15, no. 8, pp. 2226–2238, Aug. 2006.

[16] M. J. Weinberger, G. Seroussi, G. Sapiro, "The LOCO-I Lossless Image Compression Algorithm: Principles and Standardization into JPEG-LS," IEEE Trans. image Process., vol. 9, no. 8, pp. 1309–1324, 2000.

[17] X. Li, B. Yang, T. Zeng, "Efficient reversible watermarking based on adaptive prediction-error expansion and pixel selection," IEEE Trans. Image Process., vol. 20, no. 12, pp. 3524–33, Dec. 2011.